RSC Advances

ROYAL SOCIETY OF CHEMISTRY

www.rsc.org/advances

Cite this: DOI: 10.1039/c0xx00000x

www.rsc.org/xxxxxx

ARTICLE TYPE

Creation of a polymer backbone in lipid bilayer membrane-based nanotubes for morphological and microenvironmental stabilization

Yutaka Okazaki,[a] Hirokuni Jintoku,[a] Makoto Takafuji,[a] Reiko Oda[b] and Hirotaka Ihara*[ac]

Received (in XXX, XXX) Xth XXXXXXXXX 20XX, Accepted Xth XXXXXXXXX 20XX

DOI: 10.1039/b000000x

We report a novel method for morphological and microenvironmental stabilization of single-walled bilayer nanotubes, which involves construction of a polymer backbone between the monolayers by intercalating a monomer, followed by in situ polymerization.

One-dimensional nano-fabrication is becoming a key technology in various fields, including material science, electronics and biotechnology.[1] Organic nanotubes constructed by self-assembly of low-molecular-weight compounds are now particularly well staged to revolutionize nanoarchitectonics, because of their highly tunable chemical functionality and supramolecular functionality. However, despite these advantages over alternatives such as inorganic nanotubes,[2] their application is currently limited in industrial use. The primary reason is their lower stability, because their morphogenesis and functionality are based on non-covalent molecular assembling. Therefore, some approaches have been proposed to enhance their stability. For lipid bilayer membrane systems such as lipid liposomes, the first approach to stabilization (Fig. 1a) was direct polymerization of the lipids through introduction of a polymerizable group.[3] This method has been applied to drug delivery[4] and separation[5] systems. This approach is able to enhance morphological stability, but causes complete loss of certain essential properties of lipid bilayer membranes, such as lateral diffusion of lipids and phase transition behaviour between gel and liquid crystalline states. The second-generation approach to stabilization (Fig. 1b) was developed to resolve these problems.[6] By covering the ionic surfaces of lipid membranes with polymeric counter-ions, membrane stability and functionality can be considerably improved while polyionic complexation provides complex heterogeneity. This approach has been successfully applied to sensor systems.[7]

Here, we introduce a novel and facile approach as a third generation enhancement of lipid membrane stability, particularly for nanotubular aggregates. This approach (Fig. 1c) involves construction of a polymer backbone between the monolayers by intercalating monomers such as styrene or divinylbenzene, followed by in situ polymerization. It has been previously reported that the polymer thin films were prepared by template polymerization using bilayer membranes with various morphologies such as lamellar,[8] vesicles,[9] disks[10] and rods[11]. These reports mainly focused on the creation of polymer thin film-based nanostructures. In this paper, we demonstrate to stabilize chiroptical properties and morphologies of lipid bilayer membrane-based nanotubes by polymer backbone.

Certain chiral amphiphilic derivatives such as peptide-,[12] sugar-,[13] and cholesterol-containing derivatives[14] can form bilayer membrane-based nanofibrillar aggregates, including tubular structures. For this study, we focused on L-glutamide-derived lipids as a peptide-based derivative (Fig. S1), in which a functional hydrophilic group and double long chain alkyl groups as hydrophobic moieties are introduced by amide bonding into L-glutamic acid, because of their versatile tunability for chemical design and aggregate morphology.[15] In this study, *N*-pyridiniopropanoyl-L-glutamide lipid with didodecyl groups (***g*$_{12}$-Py$^+$**)†[16] was selected for creating nanotubular aggregates. ***g*$_{12}$-Py$^+$** was well dispersed in water by ultrasonication to produce clear to slightly turbid solutions. DSC measurements of the solution indicate distinct phase transition behaviour (Fig. S2). A two-step phase transition was observed during the heating process with peak top temperatures of 30 °C (T_{C1}) and 43 °C (T_{C2}), which were assigned by two kinds of crystalline (highly-ordered) states. As supporting this, unusually large Cotton effects having negative and positive signals near the absorption band of carbonyl groups were observed at temperatures below T_{C1} ($[\theta]_{200}$ = -0.9×10^5 deg cm^{-1} dmol^{-1} at 10 °C) and between T_{C1} and T_{C2} ($[\theta]_{200}$ = 1.1×10^5 deg cm^{-1} dmol^{-1} at 35 °C), respectively (Fig. S3). Furthermore, these large Cotton effects decreased markedly at temperatures above T_{C2} ($[\theta]_{200}$ = ~5.0×10^3 deg cm^{-1} dmol^{-1} at 50 °C). These results indicate that ***g*$_{12}$-Py$^+$** has different chirally stacked structures among their amide bonds below T_{C2}.

The aggregate morphology of ***g*$_{12}$-Py$^+$** was observed by transmission electron microscopy. Figure 2a shows an example prepared by casting on a copper grid and drying at 15 °C. In this procedure, temperature control was very important to obtain morphologically stable aggregates, because the aggregate morphology was dependent on the above-mentioned phase

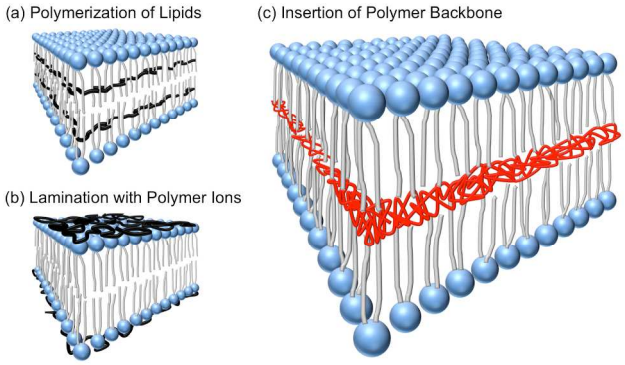

Fig. 1 Schematic illustration of lipid bilayer membranes stabilized by (a) direct polymerization of lipids, (b) covering with polymeric counter ions on ionic surfaces and (c) insertion of a polymer backbone between layers.

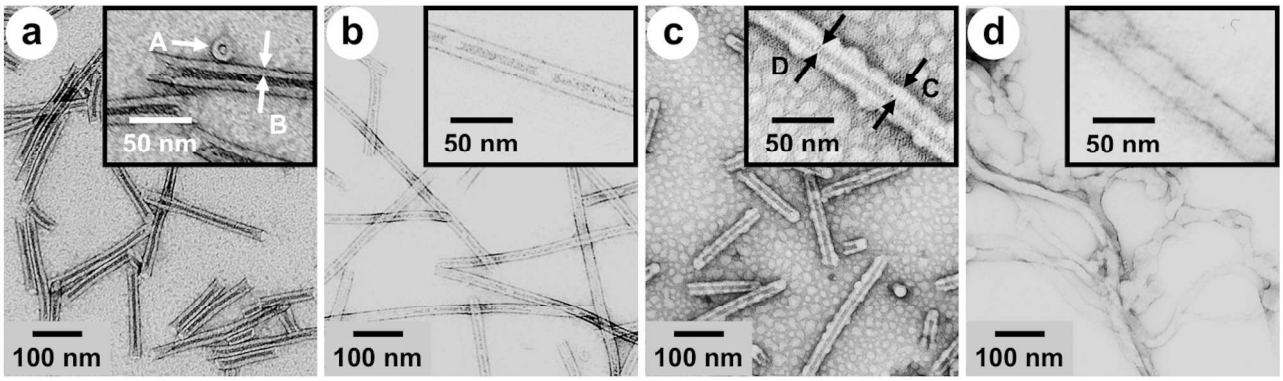

Fig. 2 TEM photographs of the g_{12}-Py^+ aggregates (a, b and c) at 15 °C and the produced polymer: (a) without monomer, (b) with styrene (100 wt% for g_{12}-Py^+), (c) with polymerized styrene-DVB (65 wt% and 35 wt% for g_{12}-Py^+), and (d) poly(styrene-DVB) after removal of g_{12}-Py^+. [g_{12}-Py^+] = 0.5 mM. All samples were stained with 1.0 wt% uranyl acetate.

transition temperature. The observed aggregates were mainly 100–400 nm in length and 17–21 nm in outer diameter. The tubular form was a torus-shaped morphology (A in Fig. 2a) at the tube terminal end. In addition, the average thickness of the white section (B in Fig. 2a) was 6.0 nm (σ = 0.65) (Fig. S6a), approximately corresponding to the bi-molecular length of g_{12}-Py^+. These results confirm that g_{12}-Py^+ forms tubular aggregates based on a single-walled bilayer membrane structure at 15 °C.

Intercalation of a polymer backbone into the bilayers (Fig. 1c) was achieved by proper selection of hydrophobic monomers and in situ polymerization. Styrene, divinylbenzene (DVB), and their mixtures are typically ideal for this purpose, while polar monomers are generally not suitable. As shown in Fig. 2b, addition of styrene to the g_{12}-Py^+ solution produced no significant alteration to the aggregate morphology, although a slight increase in diameter was observed. The tubular form was observed up to the addition of at least 400 wt% of styrene to g_{12}-Py^+. Thickness of bilayer membrane increased with increase the amount of styrene. When 100 wt% of styrene was added, the average thickness increased from 6.0 nm (σ = 0.65) to 7.0 nm (σ = 0.66) (Fig. S6).

The incorporated state of the styrene was determined by UV spectroscopy. Styrene has two peak tops (λ_{max}) at 203 and 247 nm associated with aliphatic and aromatic π–π* transitions, respectively, and their absorbance ratio A_{203}/A_{247} is influenced by microenvironmental effects such as the dielectric constant of the solvent.[10] Consistent with these properties, A_{203}/A_{247} decreased from 2.03 to 1.31 in the presence of g_{12}-Py^+ (Fig. S4), indicating that styrene was incorporated into a non-polar site.

DSC measurements provided further useful information. Addition of styrene to a g_{12}-Py^+ solution caused distinct lowering of the peak top temperatures, without any significant change in the phase transition enthalpy (Figs. 3 and S5). When 100 wt% of styrene was added to the g_{12}-Py^+ solution, T_{C2} lowered from 43 to 31 °C. However, ΔH in T_{C2}, which corresponded to the phase-transition enthalpy of alkyl chains, did not show significant difference between with and without styrene. These results suggest that styrene is mainly located (intercalated) in specific sites between the molecular layers and therefore, adding styrene does not disturb the molecular ordering or nanotubular aggregation. TEM observations and UV spectra strongly support this idea. Similar conclusions have been estimated for monomer loading of vesicular and disk-like bilayer membrane systems using small-angle neutron scattering, small-angle X-ray scattering and dynamic light scattering studies.[10,17] although no direct

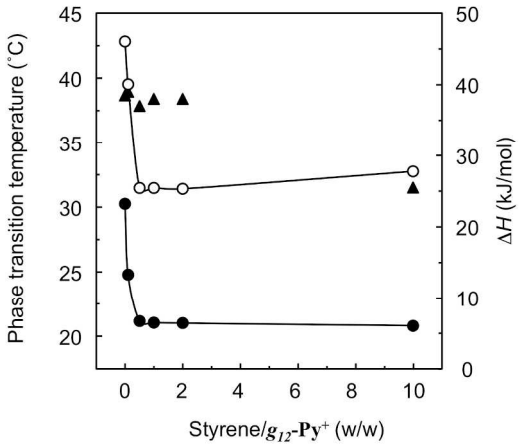

Fig. 3 Concentration dependencies of phase transition temperatures and enthalpy of the aqueous g_{12}-Py^+ solutions on styrene: T_{C1} (solid circles), T_{C2} (open circles) and ΔH in T_{C2} (solid triangles). [g_{12}-Py^+] = 20 mM.

evidence has been provided. On the other hand, addition of 4-vinylpyridine, a more hydrophilic and polar monomer, resulted in disappearance of the lower peak related to inter-hydrogen bonding interactions. These results suggest that 4-vinylpyridine is likely located near the glutamide moiety as a more hydrophilic area.

To develop a polymer backbone in the nanotubes, a styrene-DVB mixture (65:35 w/w) was incorporated into the nanotubes, and then polymerization was carried out by phtoto-initiated radical polymerization with Irgacure 369 (λ_{max} = 321 nm) at 10 °C under an ultrahigh-pressure mercury lamp with a UV cut filter.† The polymerization process was spectroscopically monitored by reduction in absorption at 247 nm assigned to the vinyl aromatic group. The original tubular morphology was completely maintained despite 99% consumption of the monomers after UV irradiation for 2 h (Fig. S7). The bilayer thickness and cavity diameter were 6–8 nm (Fig. S6) and 7–10 nm (C and D in Fig. 2c), respectively. NMR spectroscopy of the product after 2 h irradiation showed that 99% of the styrene and DVB disappeared and were converted into polymers (defined at 6.60 ppm). Evidence for polymer backbone development was also provided by characterization of the residue, from which g_{12}-Py^+ was removed by solvents such as ethanol.† Washing produced worm-like nanofibrils with diameters of 20–30 nm

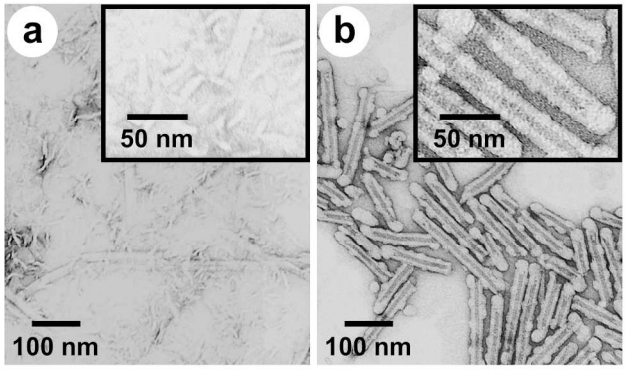

Fig. 4 TEM photographs of the g_{12}-Py^+ aggregates at 40 ˚C: (a) without any additive and (b) with polymer backbone by poly(styrene-DVB). [g_{12}-Py^+] = 0.5 mM.

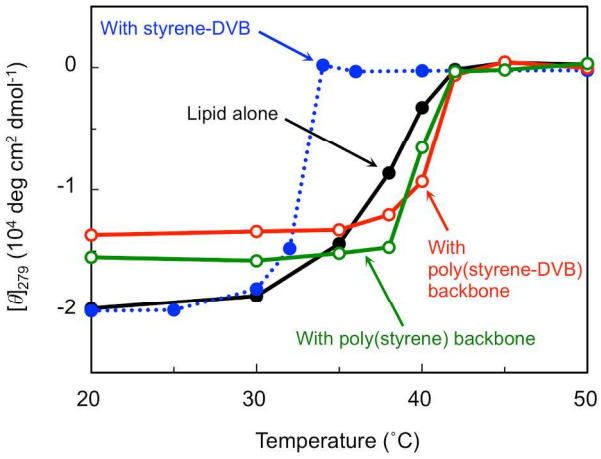

Fig. 5 Temperature dependences of $[\theta]_{279}$ indicating the highly-ordered chiral stacking states of the aqueous g_{12}-Py^+ solutions: without any additive (black line), with styrene-DVB (blue broken line), with poly (styrene) backbone (green line), and with poly(styrene-DVB) backbone (red line). [g_{12}-Py^+] = 0.5 mM, monomer/g_{12}-Py^+ = 1(w/w).

(Fig. 2d). In summary, we conclude that a polymer backbone was created within the nanotubes as illustrated in Fig. 1c.

Insertion of a polymer backbone into bilayer membrane-based nanotubes had significant positive effects on thermal stability. First, morphological stability was improved. As noted above, tubular morphology is stably produced at temperatures below T_{C1}, but becomes fragmented and helical at temperatures near T_{C2} (40 °C; Fig. 4a). However, after creating a polymer backbone, the tubular structure was maintained even at 40 °C (Fig. 4b). Supporting this result, the DSC thermogram was reversed by polymerization of the intercalated monomer; T_{C2} appeared at 40 °C, but T_{C1} nearly disappeared (Fig. S8). Second, microenvironmental structures were stabilized. The g_{12}-Py^+ aggregates showed large Cotton effects around the absorption bands for carbonyl and pyridinium groups (Fig. S3). These effects are due to chiral stacking phenomena forming secondary chirality; such specific chirality can only be observed at crystallinity temperatures.[18] Fig. 5 shows the temperature dependence of the molecular ellipticity at 279 nm $[\theta]_{279}$, which is related to the absorption band of pyridinium groups. Loading of styrene into the g_{12}-Py^+ aggregates reduced $[\theta]_{279}$, which would generally lead to disorder. However, polymerization of the intercalated styrene stabilized the chirally ordered structures.

In conclusion, we have developed a facile method for inserting a polymer backbone into lipid bilayer membrane-based nanotubes. Because the backbone does not covalently bond to lipid components, fundamental functions such as lipid mobility, molecular orientation, and unique chiroptical properties are maintained, while nanotubular morphology is also stabilized. We believe that this method is versatile for morphological and environmental stabilization of bilayer membrane-based aggregates. Further investigations with this method are in progress and the results will be published in elsewhere.

Notes and references

[a] *Department of Applied Chemistry & Biochemistry, Kumamoto University, 2-39-1 Kurokami, Chuo-ku, Kumamoto 860-8555, Japan. Fax: +81 96 3423662; Tel: +81 96 3423661; E-mail: ihara@kumamoto-u.ac.jp*

[b] *Institute of Chemistry & Biology of Membranes & Nanoobjects, UMR5248 CBMN, CNRS - Universite Bordeaux - Institut Polytechnique Bordeaux, 2 rue Robert Escarpit, 33607 Pessac, France*

[c] *Kumamoto Institute for Photo-Electro Organics (PHOENICS), 3-11-38, Higashimachi, Higashi-ku, Kumamoto, 862-0901, Japan*

† Electronic Supplementary Information (ESI) available: synthesis and characterization of g_{12}-Py^+. Experimental details: procedure of nanotube preperation, photo-initiated radical polymerization, removal of g_{12}-Py^+, sample preparation for TEM, DSC thermograms, UV-visible, circular dichroism (CD) spectra. See DOI: 10.1039/b000000x/

1 R. Karlsson, M. Karlsson, A. Karlsson, A.-S. Cans, J. Bergenholtz, B. Åkerman, A. G. Ewing, M. Voinova and O. Orwar, *Langmuir*, 2002, **18**, 4186; Y. Xia, P. Yang, Y. Sun, Y. Wu, B. Mayers, B. Gates, Y. Yin, F. Kim and H. Yan, *Adv. Mater.*, 2003, C. R. Martin and P. Kohli, *Nature Revews*, 2003, **2**, 29; **15**, 353; A. L. Briseno, S. C. B. Mannsfeld, X. Lu, Y. Xiong, S. A. Jenekhe, Z. Bao and Y. Xia, *Nano Lett.*, 2007, **7**, 668; D. M. Bassani, *Nature*, 2011, **480**, 326; C. Giansante, G. Raffy, C. Schäfer, H. Rahma, M.-T. Kao, A. G. L. Olive and A. D. Guerzo, *J. Am. Chem. Soc.* **2011**, *133*, 316; R. Tamoto, S. Lecomte, S. Si, S. Moldovan, O. Ersen, M.-H. Delville and R. Oda, *J. Phys. Chem. C*, 2012, **116**, 23143; P. Xue, J. Sun, Q. Xu, R. Lu, M. Takafuji and H. Ihara, *Org. Biomol. Chem.*, 2013, **11**, 1840; L. Macaraig, S. Chuangchote and T. Sagawa, *J. Mater. Res.*, 2014, **29**, 123.

2 S. Iijima, *Nature*, 1991, **354**, 56; M. Remskar, *Adv. Mater.*, 2004, **16**, 1497.

3 D. F. O'Brien, B. Armitage, A. Benedicto, D. E. Bennett, H. G. Lamparski, Y.-S. Lee, W. Srisiri and T. M. Sisson, *Acc. Chem. Res.*, 1998, **31**. 861; H. Ihara, M. Takafuji and T. Sakurai, *Encyclopedia of Nanosci. Nanotech.*, 2004, **9**, 473; A. Puri and R. Blumenthal, *Acc. Chem. Res.*, 2011, **44**. 1071.

4 S. L. Regen, A. Singh, G. Oehme and M. Singh, *Biochem. Biophys. Res. Commun.*, 1981, **101**, 131; J. Okada, S. Cohen and R. Langer, *Pharm. Res.*, 1995, **12**, 576.

5 C. Hirayama, H. Ihara and T. Mukai, *Macromolecules*, 1992, **25**, 6375; M. M. Rahman, M. Takafuji, H. R. Ansarian and H. Ihara, *Anal. Chem.*, 2005, **77**, 6671; A. K. Mallik, H. Qiu, T. Sawada, M. Takafuji and H. Ihara, *Anal. Chem.*, 2012, **84**, 6577.

6 N. Nakashima, K. Yamashita, T. Jorobata, K. Tanaka, K. Nakano and M. Takagi, *Anal. Sci.*, 1986, **2**, 589; L. Zhang, M. L. Longo and P. Stroeve, *Langmuir*, 2000, **16**, 5093.

7 Y. Okahata, H. Ebato and K. Taguchi, *J. Chem. Soc., Chem. Commun.*, 1987, **18**, 1363; K. Hayashi, K. Yamafuji, K. Toko, N. Ozaki and T. Yoshida, *Sensors and Actuators*, 1989, **16**, 25; N. Nakashima, Y. Yamaguchi, H. Eda, M. Kunitake and O. Manabe, *J. Phys. Chem. B*, 1997, **101**, 215.

8 J. Wu, J. H. Harwell and E. A. O'Rear, *Langmuir*, 1987, **3**, 531; J. Wu, J. H. Harwell and E. A. O'Rear, *Langmuir*, 1987, **91**, 623.

9 J. Kurja, R. J. M. Nolte, I. A. Maxwell and A. L. German, *Polymer*, 1993, **34**, 2045; J. D. Morgan, C. A. Johnson and E. W. Kaler, Langmuir, 1997, **13**, 6447; M. Jung, D. H. W. Hubert, P. H. H. Bomans, P. M. Frederik, J. Meuldijk, A. M. van Herk, H. Fischer and A. L. German, *Langmuir*, 1997, **13**, 6877.

10 S. Tekobo and E. Pinkhassik, *Chem. Commun.*, 2009, 1112.

11 F. Becerra, J. F. A. Soltero, J. E. Puig, P. C. Schulz, J. Esquena and C. Solans, *Colloid polym. Sci.*, 2003, **282**, 103.

12 T. Imae, Y. Takahashi and H. Muramatsu, *J. Am. Chem. Soc.*, 1992, **114**, 3414; Q. Cheng, M. Yamamoto and R. C. Stevens, *Langmuir*, 2000, **16**, 5333; M. K. Baumann, M. Textor and E. Reimhult, *Langmuir*, 2008, **24**, 7645.

13 F. Reichel, A. M. Roelofsen, H. P. M. Geurts, S. J. Gaast, M. C. Feiters and G.-J. Boons, *J. Org. Chem.*, 2000, **65**, 3357; J. H. Jung, G. John, K. Yoshida and T. Shimizu, *J. Am. Chem. Soc.*, 2002, **124**, 10674; T.-F. Lin, R.-M. Ho, C.-H. Sung and C.-S. Hsu, *Chem. Mater.*, 2008, **20**, 1404.

14 I. Cho and J. G. Park, *Chem. Lett.*, 1987, 977; D. S. Chong, G. B. Benedek, F. M. Konikoff and J. M. Donovan, *Proc. Natl. Acad. Sci. USA*, 1993, **90**, 11341; P. Terech, A. Geyer, B. Struth and Y. Talmon, *Adv. Mater.*, 2002, **14**, 495.

15 K. Yamada, H. Ihara, T. Ide, T. Fukumoto and C. Hirayama, *Chem. Lett.*, 1984, 1713; T. Hatano, A.-H. Bae, M. Takeuchi, N. Fujita, K. Kaneko, H. Ihara, M. Takafuji and S. Shinkai, *Angew. Chem. Int. Ed.*, 2004, **43**, 465; Y. Li and M. Liu, *Chem Commun* 2008, 5571.

16 H. Ihara, M. Takafuji, C. Hirayama and D. F. O'Brien, *Langmuir* 1992, ***8***, 1548.

17 A. G. Richter, S. A. Dergunov, B. Ganus, Z. Thomas, S. V. Pingali, V. Urban, Y. Liu, L. Porcar and E. Pinkhassik, *Langmuir*, 2011, **27**, 3792.

18 H. Ihara, H. Hachisako, C. Hirayama and K. Yamada, *Liquid Cristals*, 1987, **2**, 215.